Introduction

Microseisms from hydraulic fracturing occur in the Earth at unknown locations and times, but we want to image the locations of the microseisms to gather information about how effective the hydraulic fracturing process was. Previous work on finding the hypocenter (origin location and time) of microseisms has focused on extending conventional techniques from earthquake seismology to microseisms by picking P and S arrival times and then triangulating the hypocenter location given a velocity model and the differences in the P and S arrival times at multiple receivers (Bancroft et al., 2010; Kummerow, 2010; Bose et al., 2009; Eisner et al., 2008; Lu et al., 2008). While these efforts have been mostly successful, ultimately we would like to find microseism hypocenters without having to pick event arrivals, because picking algorithms may fail in noisy datasets (Bose et al., 2009; Eisner et al., 2008). In these situations, useful information is discarded during imaging because microseismic events are not recognized by the picking algorithm.

An alternative approach that avoids picking event arrivals, is to use reverse-time imaging to locate the events by refocusing their reconstructed wavefields at some point in space, x_0, and some time, t_0 (Artman et al., 2010; Saenger and Kocur, 2010; Steiner and Saenger, 2010; Witten and Artman, 2010; Xuan and Sava, 2010; Lu et al., 2008; Gajewski et al., 2007; Rentsch et al., 2007). However this approach has a significant shortcoming because we do not find the hypocenter location merely by focusing the wavefield. In addition, we need to explore the wavefield looking for objects that represent focused events or implement an imaging condition to produce an image of the microseisms. To our knowledge, there have been only a handful of attempts at automatic focus detection, because the problem is a difficult computer vision problem (Xuan and Sava, 2010). Instead, almost all work has focused on implementing various imaging conditions (Artman et al., 2010; Gajewski et al., 2007; Rentsch et al., 2007; Sava and Poliannikov, 2007; Borcea et al., 2006). Along the same lines, we propose a new imaging condition that uses additional information about the geometry of our receiver arrays and the spatio-temporal coincidence of the wavefield at the hypocenter location to image microseisms.

Theory

The fundamental idea we use in our method is that when we have the correct velocity for wavefield extrapolation, that the wavefield from all receivers arrives at the spatio-temporal location for the microseism simultaneously but from distinctly different paths. Thus, if we reconstruct the wavefield (by time-reversal) for small groups of receivers that have distinctly different angular aperture, then their reconstructed wavefields do not coincide in space and time until they are at the hypocenter of the microseism. To capture the actual coincidence of the wavefields at the right point in space-time, we apply the zero-lag cross-correlation (multiplication) imaging condition to all of the reconstructed wavefields together for each time-step to produce a hyper-dimensional "image" as a function of space and time. Formally this process is described as,

$$R(\mathbf{x},t) = \prod_{i=1}^{N_G} W_R^i(\mathbf{x},t) = \prod_{i=1}^{N_G} \sum_{j=1}^{N_R} U_R^j(\mathbf{x},t), \tag{1}$$

where R is the event "image", N_G is the number of receiver groups that we arbitrarily choose to create, W_R^i is the reconstructed wavefield for the i^{th} receiver group, U_R^j is the reconstructed wavefield for the j^{th} receiver, N_R is the number of receivers in the i^{th} receiver group and $\mathbf{x}$ and t are the space and time coordinates, respectively. The total number of receivers N_R^{total} is equal to the sum of N_R over all groups. If the number of receivers per group is equal then $N_R^{total} = N_R N_G$. Additionally, we sum the image R over all time in equation 1 to produce a spatial image, M, of microseismic event locations over all time as follows,

$$M(\mathbf{x}) = \sum_t R(\mathbf{x},t) \tag{2}$$

Equation (1) raises two important questions: how do we decide how many groups of receivers, N_G to use and how do we determine which receivers to group together. To answer the first question, we consider two special cases of equation 1. In the first case we let $N_G = 1$, which causes the wavefield

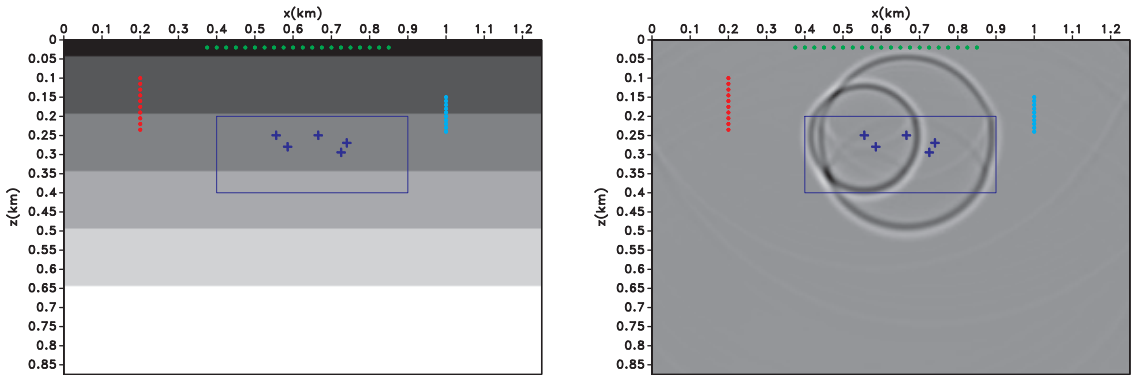

(a) (b)

Figure 1: The source and receiver geometry for the synthetic microseismic experiment overlain on the velocity model (a). The receivers are in two boreholes and near the surface. The microseismic hypocenters (crosses) occur randomly in the reservoir of interest at random times over a four second interval as the wavefield snapshot at $t = 2.65$ seconds shows (b).

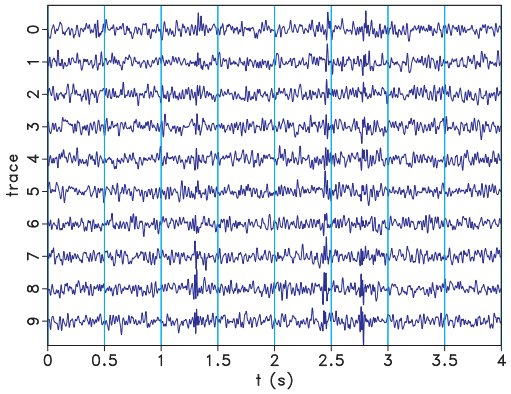

Figure 2: The synthetic data with strong, bandlimited random noise added for the borehole at $x = 0.2$ km. The microseisms arrive near the following times (in seconds): 1.5, 2.4, 2.5, 2.7, 2.8, but are barely visible because of the strong noise which makes picking arrivals nearly impossible.

from each receiver to be summed together into one wavefield as we would do for conventional reverse-time imaging. By letting $N_G = 1$, there is only one wavefield reconstruction, but we have removed the product from equation 1, and therefore removed our ability to locate events by wavefield triangulation. Conversely, if we let N_G equal the number of receivers N_R^{total} (i.e. each receiver is its own group), then we have to reconstruct the wavefield using reverse-time propagation for each receiver independently, which is prohibitively expensive. However, each additional receiver group increases the resolution of the resultant image because the spatio-temporal correlation for all receivers is maximum at the hypocenter location. Subsequently, the sensitivity of this method to errors in the velocity model and noise increases as the number of receiver groups increases. In regards to the second question, we group receivers together that have similar angular aperture. The limits of what constitutes similar aperture are arbitrary, but the goal should be to maximize the difference in angular aperture between the separate groups of receivers so as to decrease the spatio-temporal correlation of receiver groups.

We note the similarity between this approach and triangulation (Bancroft et al., 2010). In fact, this method is triangulation when $N_G = N_R^{total}$ but without arrival time picking. In most circumstances $1 < N_G < N_R^{total}$, which puts our proposed method between triangulation and reverse-time imaging, which means that the method inherits some of the beneficial attributes of both methods: i.e. improved SNR and resolution.

Synthetic example

To demonstrate this idea, consider the following synthetic example with receivers in two separate boreholes on the outskirts of a zone of interest in a reservoir and more receivers on the surface of the Earth, as shown in Figure 1(a). For simplicity, we assume that the Earth is acoustic with a $v(z)$ velocity model.

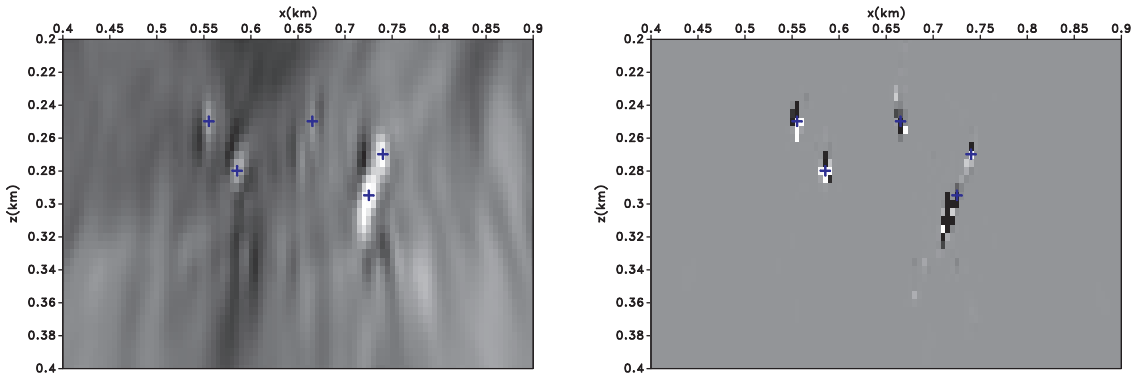

(a) (b)

Figure 3: The spatial map $M(\mathbf{x})$ of the microseismic hypocenters for both experiments, $N_G = 3$ (left) and $N_G = N_R^{total}$ (right). We only show the map for the boxed area in Figure 1(a). The crosses indicate the actual hypocenters of the microseisms. For fewer receiver groups (left), the resultant image consists of "blobs" that indicate the hypocenter location. When we use more receiver groups (right) the "blobs" are better resolved. Notice how the peak of the blobs corresponds with the actual hypocenter location. The images for both experiments are contaminated by noise, which makes it more difficult to uniquely identify microseism hypocenters. For example, the image for three receiver groups (left) is contaminated by low-level noise present in the entire image. The image for all receivers (right) is contaminated by a strong, spurious event at $(x = 0.7, z = 0.32)$ km that could be interpreted as another microseism.

We synthesize five microseisms over four seconds at various locations to produce data at the receivers. We then conduct two experiments: one in which we segment the receivers into three separate groups, $N_G = 3$ and another in which we treat each receiver as its own group $N_G = N_R^{total}$. In the first experiment we combine the receivers into the following groups: the receivers in the borehole at $x = 0.2$ km, the receivers on the surface, and the receivers in the borehole at $x = 1.0$ km. We add strong bandlimited noise in the band of our synthetic microseisms to our data to simulate the effect of noisy acquisition, Figure 2. We time-reverse the data for each receiver group and then propagate it using the *correct* velocity model. After propagation, we apply the imaging condition from equation 1 and then stack the image over time to produce a spatial map of microseismic events as in Figures 3(a) - 3(b). Additionally, we could scan the image over time to find the time of origin of the microseisms by threshholding.

Discussion

The predicted and actual locations of the microseisms are shown for both experiments in Figures 3(a) - 3(b). In both cases, the presence of strong noise corrupts the image and creates spurious events. The images show the location of the microseisms, although the resolution of the locations are different for the two experiments. In the first experiment, where $N_G = 3$, the hypocenters are smeared in space. It appears that the spatial smearing is caused by two phenomena: receiver aperture, and the wavefields from the separate receiver groups strongly correlating in the vicinty of the hypocenter. The strong correlation is most likely the result of the wavefields having similar angular aperture near the hypocenter. The effects of receiver aperture are unavoidable, but we hypothesize that the lack of immediate defocusing can be exploited for incorrect velocity models, because the events still produce significant enough correlations to be apparent in the image. For the second experiment, $N_G = N_R^{total}$ the resolution is greatly improved as the hypocenters are basically points in space. However, this configuration is more sensitive to noise, as indicated by the presence of spurious events in Figure 3(b) near $(x = 0.7, z = 0.32)$ km, and/or velocity errors because a single bad trace could destroy the correlation between the wavefields from the different receivers. For example, if we have a dead trace (all-zeros) from a single receiver, then the reconstructed wavefield is zero everywhere in space and time, and the product of this wavefield with

the wavefields from other receivers is zero, even if all other wavefields indicate that a microseism is present at a particular location. To avoid this issue, we could also decrease the number of receiver groups N_G, thereby increasing the number of receivers per group N_R, which would improve the SNR of a single receiver group by summation of nearby wavefields. Alternatively, we could use a more intelligent imaging condition that only produces an image at some location in space and time if a certain number of wavefields from different receiver groups agree (i.e. have a similar value at a location in space and time). We hypothesize that allowing the wavefields to "vote" would greatly improve the SNR in even the noisiest datasets, but leave the implementation of this idea for future research.

Conclusions

We present a method for locating microseism hypocenters in both space and time, by correlating multiple reconstructed wavefields corresponding to different groups of receivers. The method is mathematically and conceptually similar to triangulation, but does not require arrival picking. Additionally, this method allows one to trade computational cost with spatial and temporal resolution by changing the number of receiver groups to use. The major downside to this method is computational cost because reverse-time imaging for a number of receiver groups is more computationally expensive than imaging data from all receivers at once.

REFERENCES

Artman, B., I. Podladtchikov, and B. Witten, 2010, Source location using time-reverse imaging: Geophysical Prospecting, **58**, 861–873.

Bancroft, J. C., J. Wong, and L. Han, 2010, Sensitivity of locating of a microseismic event when using analytic solutions and the first arrival times: SEG Technical Program Expanded Abstracts, **29**, 2191–2195.

Borcea, L., G. Papanicolaou, and C. Tsogka, 2006, Coherent interferometric imaging in clutter: Geophysics, **71**, SI165–SI175.

Bose, S., H. P. Valero, Q. Liu, R. G. Shenoy, and A. Ounadjela, 2009, An automatic procedure to detect microseismic events embedded in high noise: SEG Technical Program Expanded Abstracts, **28**, 1537–1541.

Eisner, L., D. Abbott, W. B. Barker, J. Lakings, and M. P. Thornton, 2008, Noise suppression for detection and location of microseismic events using a matched filter: SEG Technical Program Expanded Abstracts, **27**, 1431–1435.

Gajewski, D., D. Anikiev, B. Kashtan, E. Tessmer, and C. Vanelle, 2007, Localization of seismic events by diffraction stacking: , 1287–1291.

Kummerow, J., 2010, Using the value of the crosscorrelation coefficient to locate microseismic events: Geophysics, **75**, MA47.

Lu, R., M. N. Toksoz, and M. E. Willis, 2008, Locating microseismic events with time reversed acoustics: A synthetic case study: , 1342–1346.

Rentsch, S., S. Buske, S. Luth, and S. A. Shapiro, 2007, Fast location of seismicity: A migration-type approach with application to hydraulic-fracturing data: Geophysics, **72**, S33.

Saenger, E. H., and G. K. Kocur, 2010, Time reverse characterization of sources in 2D and 3D heterogeneous media: SEG Technical Program Expanded Abstracts, **29**, 2049–2053.

Sava, P., and O. Poliannikov, 2007, Interferometric imaging condition for wave-equation migration: SEG Technical Program Expanded Abstracts, **26**, 2330–2334.

Steiner, B., and E. H. Saenger, 2010, Comparison of 2D and 3D time reverse modeling for tremor source localization: SEG Technical Program Expanded Abstracts, **29**, 2171–2175.

Witten, B., and B. Artman, 2010, Signal-to-noise estimates of time-reverse images: SEG Technical Program Expanded Abstracts, **29**, 2176–2180.

Xuan, R., and P. Sava, 2010, Probabilistic microearthquake location for reservoir monitoring: Geophysics, **75**, MA9–MA26.